

Multiplexed CRISPR-Cas9 based genome editing of *Rhodospiridium toruloides*

**Peter B. Otoupal,^{a,b} Masakazu Ito,^{c,d} Adam P. Arkin,^{e,f,g} Jon K. Magnuson,^{a,h} John
M. Gladden,^{a,b} & Jeffrey M. Skerker^{d,f,g}**

^aJoint BioEnergy Institute, Emeryville, California, USA

^bBiomass Science and Conversion Technologies, Sandia National Laboratories, Livermore, California, USA

^cT-Frontier Division, Frontier Research Center, Toyota Motor Corporation, Aichi, Japan

^dEnergy Biosciences Institute, Berkeley, California, USA

^eEnvironmental Genomics and Systems Biology Division, Lawrence Berkeley National Laboratory, Berkeley, California, USA

^fBiological Systems and Engineering Division, Lawrence Berkeley National Laboratory, Berkeley, California, USA

^gDepartment of Bioengineering, University of California, Berkeley, Berkeley, California, USA

^hChemical and Biological Processing Group, Pacific Northwest National Laboratory, Richland, Washington, USA

Address correspondence to Peter B. Otoupal, Potopua@Sandia.GOV, or Jeffrey M. Skerker, skerker@berkeley.edu

1 **ABSTRACT**

2 Microbial production of biofuels and bioproducts offers a sustainable and economic
3 alternative to petroleum-based fuels and chemicals. The basidiomycete yeast
4 *Rhodospiridium toruloides* is a promising platform organism for generating bioproducts
5 due to its ability to consume a broad spectrum of carbon sources (including those derived
6 from lignocellulosic biomass) and to naturally accumulate high levels of lipids and
7 carotenoids, two biosynthetic pathways that can be leveraged to produce a wide range of
8 bioproducts. While *R. toruloides* has great potential, it has a more limited set of tools for
9 genetic engineering relative to more advanced yeast platform organisms such as
10 *Yarrowia lipolytica* and *Saccharomyces cerevisiae*. Significant advancements in the past
11 few years have bolstered *R. toruloides*' engineering capacity. Here we expand this
12 capacity by demonstrating the first use of CRISPR-Cas9 based gene disruption in *R.*
13 *toruloides*. Stably integrating a Cas9 expression cassette into the genome brought about
14 successful targeted disruption of the native *URA3* gene. While editing efficiencies were
15 initially low (0.002%), optimization of the cassette increased efficiencies 364-fold (to
16 0.6%). Applying these optimized design conditions enabled disruption of another native
17 gene involved in carotenoid biosynthesis, *CAR2*, with much greater success; editing
18 efficiencies of *CAR2* deletion reached roughly 50%. Finally, we demonstrated efficient
19 multiplexed genome editing by disrupting both *CAR2* and *URA3* in a single
20 transformation. Together, our results provide a framework for applying CRISPR-Cas9 to
21 *R. toruloides* that will facilitate rapid and high throughput genome engineering in this
22 industrially relevant organism.

23 **IMPORTANCE**

24 Microbial biofuel and bioproduct platforms provide access to clean and renewable carbon
25 sources that are more sustainable and environmentally friendly than petroleum-based
26 carbon sources. Furthermore, they can serve as useful conduits for the synthesis of
27 advanced molecules that are difficult to produce through strictly chemical means. *R.*
28 *toruloides* has emerged as a promising potential host for converting renewable
29 lignocellulosic material into valuable fuels and chemicals. However, engineering efforts
30 to improve the yeast's production capabilities have been impeded by a lack of advanced
31 tools for genome engineering. While this is rapidly changing, one key tool remains
32 unexplored in *R. toruloides*; CRISPR-Cas9. The results outlined here demonstrate for the
33 first time how effective multiplexed CRISPR-Cas9 gene disruption provides a framework
34 for other researchers to utilize this revolutionary genome-editing tool effectively in *R.*
35 *toruloides*.

36

37

38 **KEYWORDS**

39 *Rhodospiridium toruloides*, CRISPR-Cas9, genome engineering, multiplexed, *URA3*,
40 *CAR2*, tRNA

41 *Rhodospiridium toruloides* (also known as *Rhodotorula toruloides*) is a basidiomycetous
42 yeast that has attracted interest for its great bioengineering potential. The oleaginous
43 yeast can be readily cultivated in high-density cell cultures (1), and naturally accumulates
44 large quantities of both carotenoids and lipids (2) which serve as precursors for many
45 valuable compounds. Complementing this is the ability of *R. toruloides* to efficiently
46 consume a wide variety of carbon sources, including those found in lignocellulose
47 hydrolysates (3, 4). Furthermore, *R. toruloides* can grow robustly under difficult
48 environmental conditions including high osmotic stress (5) and the presence of ionic
49 liquids used in pretreatment processes (6–8). It is therefore being assessed as a novel
50 platform for the industrial-scale generation of valuable commodities including biofuels,
51 pharmaceuticals, and other advanced bioproducts (9–12).

52 Despite these advantages, commercial adoption of *R. toruloides* will be hampered
53 until effective genetic engineering tools are developed in this system (13–15). Notably,
54 no autonomously replicating sequences (ARS) have been identified for use in *R.*
55 *toruloides*, meaning that all genetic manipulation of this organism to date has been
56 accomplished by direct integration of heterologous DNA elements into the genome. The
57 genetic engineering toolkit for *R. toruloides* has been expanded in recent years with the
58 development of transformation techniques such as *Agrobacterium tumefaciens*-mediated
59 transformation (16) (ATMT), electroporation (15, 17) and lithium acetate chemical
60 transformation (14), which have enabled both efficient random integration based on the
61 non-homologous end joining (NHEJ) pathway, and targeted deletion/integration based on
62 homologous recombination (HR) (18, 19),

63 Concurrent with these advances is a revolution in the field of genome engineering
64 brought on by the development of precise genome and transcriptome editing through
65 clustered regularly interspaced short palindromic repeat (CRISPR)-based systems (20–
66 22). Modern genetic engineering approaches in other organisms have largely gravitated
67 towards using CRISPR systems to enact desired DNA changes (23–25). This approach
68 utilizes a ribonucleoprotein complex (RNP) consisting of a CRISPR associated nuclease
69 (Cas, the most common being Cas9) and a synthetic single guide RNA (sgRNA). The
70 sgRNA contains a ~20 nucleotide (nt) spacer sequence complementary to a unique DNA
71 sequence in the targeted organism, as well as a 76 nt handle that complexes with Cas9.
72 By modifying the 20 nt spacer sequence of the sgRNA, researchers can direct the
73 nuclease to a specific location and enact targeted DNA cleavage.

74 While CRISPR-Cas9 has revolutionized the world of genome editing, it has yet to
75 be demonstrated in *R. toruloides*. The yeast's potential as a robust host for the production
76 of bioproducts would be significantly improved by the development of CRISPR-Cas9
77 strategies for engineering its genome, especially considering that the genetic engineering
78 toolkit for *R. toruloides* has fallen behind that of more developed yeasts such as *Yarrowia*
79 *lipolytica* (26–29). Cas9 engineering is more amenable to multiplexed gene editing than
80 the current techniques for manipulating *R. toruloides*' genome based on ATMT (30).
81 Furthermore, CRISPR-Cas edits can be employed in a matter of days (31), while ATMT
82 gene editing can take anywhere from two weeks to one month (16). Another advantage
83 of CRISPR-Cas9 gene editing is that it can utilize NHEJ to create site-specific gene
84 deletions, while current techniques relying on HR via *KU70* deletion of the NHEJ repair
85 pathway suffer from the apparent low activity of HR repair relative to NHEJ in *R. toruloides*

86 (15, 32). Targeted gene disruptions would likely be more easily accomplished utilizing
87 CRISPR-Cas9 targeting followed by error-prone NHEJ repair than the current approach.
88 Here we demonstrate the first application of gene editing using CRISPR-Cas9 in
89 *R. toruloides*. Genomic integration of the coding sequences of Cas9 and an associated
90 sgRNA allows for targeted gene disruption of *URA3* upon (likely NHEJ-based) repair of
91 DNA cleavage. Although initial editing efficiency was low ($0.0017\% \pm 0.0011\%$),
92 optimizing expression of the sgRNA and fine-tuning of its target sequence led to a 364-
93 fold improvement in editing success of up to $0.62\% \pm 0.50\%$. Using the design principles
94 learned in targeting *URA3*, we developed CRISPR-Cas9 constructs to disrupt the
95 carotenoid biosynthesis gene, *CAR2*. Attempts to delete this gene resulted in significantly
96 greater success, with editing efficiencies reaching up to $46 \pm 22\%$ of all cells transformed
97 with the CRISPR-Cas9 expression cassette. We further show that multiplexed gene
98 disruption of the *R. toruloides* genome is possible using this approach. Combining an
99 array of four sgRNAs separated by self-processing tRNA elements successfully allowed
100 for targeted deletions of both *CAR2* and *URA3* in one simultaneous transformation. We
101 observed both indels near each cut site and complete deletion of the region between the
102 cut sites. We demonstrate that by using two sgRNAs to disrupt each gene, the intergenic
103 region between these two cut sites can be excised during the DNA repair process.
104 Interestingly, *R. toruloides* demonstrated a propensity to re-insert the excised DNA in its
105 reverse orientation, further supporting the observation that the organism is particularly
106 effective at accomplishing NHEJ-based DNA repair. Taken together, these results outline
107 a strategy for achieving efficient CRISPR-based genome editing in *R. toruloides* and will
108 streamline metabolic engineering efforts in this industrially relevant organism.

109 **RESULTS**

110 **Integration of Cas9 and sgRNA into *R. toruloides*' genome allows for targeted gene**
111 **disruption.** We first designed a Cas9 expression construct for use in *R. toruloides*. This
112 included codon optimization, addition of a nuclear localization sequence (NLS) to Cas9,
113 and selection of the native GAPDH promoter for constitutive expression. An sgRNA
114 expression cassette was placed upstream of the Cas9 sequence cassette consisting of a
115 promoter, a hepatitis delta virus (HDV) ribozyme cleavage sequence, a 20 nt unique gene
116 targeting sequence, a 76 nt common sgRNA handle for the association of Cas9 with the
117 RNA, and a terminator sequence. The SNR52 RNA polymerase III promoter and
118 terminator sequences from *Saccharomyces cerevisiae* were employed to drive
119 expression of this sgRNA, as they have been used successfully in other fungi (33, 34).
120 Placing a ribozyme element between the SNR52 promoter and the sgRNA element
121 resulted in improved editing efficiency in *S. cerevisiae* in our previous work (35). The
122 ribozyme was therefore included in the hopes of increasing editing efficiency in *R.*
123 *toruloides*.

124 To validate this CRISPR-Cas9 system, the *URA3* gene encoding orotidine 5'-
125 phosphate decarboxylase was targeted for deletion. Expression of the decarboxylase is
126 known to allow yeast to convert 5-fluoroorotic acid (5-FOA) into 5-fluorouracil, a
127 compound that is highly toxic to most yeast (36). Therefore, successful editing (i.e. loss
128 of function of *URA3* caused by error-prone NHEJ repair of the Cas9-mediated dsDNA
129 break) can be selected for by growth in the presence of 5-FOA.

130 The first attempt to generate edits at the *URA3* locus was done in a single-step by
131 transforming a PCR fragment containing both the Cas9 and a *URA3*-specific sgRNA

132 expression cassette, followed by selection on 5-FOA plates (Fig. 1A). The number of 5-
133 FOA resistant (*5-FOA^R*) colonies obtained in the presence of the Cas9/sgRNA cassette
134 was indistinguishable from a control transformation in the absence of the PCR fragment,
135 suggesting that editing, if it occurred, was no more frequent than the rate of spontaneous
136 *5-FOA^R* (Fig. 1B). Sequencing DNA from three *5-FOA^R* colonies near the cut site of Cas9
137 revealed a consistent frame shift occurred outside of the target sequence (Fig. 1C). This
138 suggests that *5-FOA^R* arose not from Cas9-mediated gene disruption, but through
139 spontaneous mutation of *URA3* leading to loss of function. We thought that this failure in
140 Cas9-based gene editing may have been due to poor expression of the sgRNA from the
141 non-native SNR52 promoter sequence, or due to targeting an area of the genome not
142 amenable to Cas9 binding. However, even upon replacing the SNR52 promoter with four
143 other variants, and utilizing an alternative sgRNA, no improvement in 5-FOA colony
144 formation was observed (Fig. S1). Indeed, each of these variants resulted in the same
145 spontaneous mutation outside of the Cas9 cut site (Fig. S1).

146 It was hypothesized that this failure of Cas9-mediated gene editing was due to
147 insufficient expression of the CRISPR machinery during the transformation process. To
148 alleviate this problem, a new approach was employed in which the CRISPR cassette was
149 first targeted for stable integration using a selectable drug marker cassette that encodes
150 for nourseothricin resistance (*NAT^R*) before screening for successful *URA3* editing (Fig.
151 1D).

152 Approximately 300 *NAT^R* colonies were obtained after transformation and three
153 colonies were selected for subsequent screening of Cas9-mediated DNA editing. Growing
154 each colony in YPD followed by plating on YPD supplemented with 5-FOA resulted in 93

155 ± 40 colonies (Fig. 1E). A control transformation of *NAT^R* without the CRISPR cassette
156 resulted in significantly fewer spontaneously 5-FOA^R colonies (1.6 ± 0.5) This was
157 significantly above the background level of spontaneous 5-FOA resistance observed
158 utilizing the same process in the control transformation with no PCR DNA ($P = 0.02$).
159 Furthermore, sequencing revealed indels near the cut site that resulted in frameshifts,
160 suggesting that error-prone NHEJ repair occurred in a specific location dictated by the
161 sgRNA sequence (Fig. 1F). Utilizing the other four promoter variants also resulted in
162 successful gene disruption at the Cas9 cut site (Fig. S2).

163 These results indicate that stable integration of a Cas9-sgRNA expression
164 cassette into the genome allows for successful gene editing in *R. toruloides*. Additionally,
165 growth curves of wild-type cells and cells harboring the Cas9-sgRNA cassette show no
166 difference in growth rates, indicating that the cassette does not elicit detrimental fitness
167 effects (Fig. S3). However, while the CRISPR-Cas9 system was able to disrupt genes,
168 the efficiency of this process was low. The efficiency of gene editing was determined by
169 comparing the total amount of colony forming units (CFUs) in the presence of 5-FOA to
170 CFUs in the absence of 5-FOA. Total colony forming units were roughly 10^5 -fold higher
171 in the absence of 5-FOA, indicating that Cas9 editing efficiency was on the order of
172 $\sim 0.001\%$. Due to this overall low editing efficiency, focus shifted to the optimization of
173 editing efficiency. Initial tests attempting to improve Cas9-editing by adding an additional
174 NLS resulted in a decrease in editing efficiency (Fig. S4), so improvement in the design
175 of the sgRNA sequence was pursued in the following experiments.

176

177 **sgRNA target optimization.** The first point of optimization in the sgRNA design
178 was to re-consider the 20nt DNA targeting sequence used in the sgRNA. Complex
179 secondary structure near the DNA target sequence can lead to significant hindrance to
180 Cas9 activity (37). Therefore, the program sgRNA Scorer 2.0 was used to optimize target
181 sequences of Cas9 (38). This program is based on sgRNA design principles uncovered
182 in human cell lines, and while it has been utilized to design successful sgRNAs for Cas9
183 editing in yeast (39), its applicability outside of human cell lines is not well-known.
184 Therefore, seven new target sequences for *URA3* were selected representing a range of
185 different predicted scores and a series of new editing constructs were generated
186 (plasmids 213-233, Table S1) to test their relative editing efficiency. Altering the sgRNA
187 targeting sequence had a noticeable impact on editing efficiency. In the optimal case,
188 editing efficiency was improved ~14-fold over the original sgRNA target sequence, while
189 the sgRNA predicted to perform worst reduced editing efficiency ~9-fold (Fig. 2A). This
190 indicates that sgRNA target optimization is important for achieving acceptable levels of
191 editing efficiency in *R. toruloides*, and that established design tools can facilitate
192 construction of new sgRNA targets.

193 Another point of optimization was the ribozyme included between the sgRNA
194 promoter and the 20nt guide sequence. The ribozyme was originally included for its
195 potential to protect the 5' end of the sgRNA from 5' exonucleases, and was found to aid
196 in improving editing efficiencies in *S. cerevisiae* (35, 40). The ribozyme was removed to
197 see if this was the case. This alteration caused the editing efficiency to increase 26-fold
198 (Fig. 2B), significantly improving Cas9-directed gene editing ($P = 0.004$). As such, we

199 recommend the exclusion of the 5' HDV ribozyme in designing sgRNAs for expression in
200 *R. toruloides*.

201 Alternatives to the promoter sequence used in driving sgRNA expression were
202 explored next. A variety of RNA Pol-III promoters were examined, each excluding the
203 detrimental ribozyme element. The original SNR52 promoter used here, which was
204 originally derived from *S. cerevisiae*, was replaced with an analogous SNR52 promoter
205 element from another oleaginous yeast, *Y. lipolytica*, as this sequence has been proven
206 to produce functional sgRNAs in other systems (41). However, this change made no
207 significant impact on editing efficiency (Fig. 2C). Since it is unknown if SNR52 exists in
208 *R. toruloides*, a native SNR52 sequence for driving sgRNA expression could not be used.

209 To utilize a native *R. toruloides* sequence, we turned to an alternative promoter
210 system to drive sgRNA expression. Work in other fungi has found that tRNAs can serve
211 as promoters for sgRNAs *in vivo* (35, 42). Furthermore, tRNAs contain internal elements
212 that promote RNase P and Z mediated cleavage at specific sites, allowing for formation
213 of precise final sgRNA sequences. Including the *R. toruloides* tRNA^{Tyr} sequence
214 downstream of the *S. cerevisiae* SNR52 promoter increased editing efficiency slightly
215 (1.8-fold), but significantly ($P = 0.02$) (Fig. 2C). Furthermore, directly replacing the SNR52
216 promoter with tRNAs led to successful editing. This was particularly true of tRNA^{Phe} and
217 tRNA^{Tyr}, whose use as sgRNA promoters led to editing efficiencies 14-fold and 13-fold
218 greater, respectively (or $0.62\% \pm 0.50\%$ and $0.59\% \pm 0.34\%$ editing efficiency,
219 respectively). These results indicate that native *R. toruloides* tRNA promoters are more
220 effective than heterologous SNR52 promoters for Cas9-based gene editing. This could
221 be due to increased sgRNA expression, although this remains to be tested.

222

223 **Multiplexed gene disruption with CRISPR Cas9.** In order to develop a multiplex
224 gene editing system for *R. toruloides*, a second target gene was selected, *CAR2*, a gene
225 that encodes for a phytoene synthase/lycopene cyclase protein that is essential for
226 carotenoid biosynthesis (43). Loss of *CAR2* function is easily observed as a change in
227 colony color from red to white.

228 A set of single guides targeting *CAR2* were first designed to disrupt the *CAR2* locus
229 and their editing efficiencies tested. Four different Cas9-sgRNA-*NAT^R* constructs were
230 built using the design principles discovered for *URA3* editing and transformed into *R.*
231 *toruloides*. After stable integration using the *NAT^R* selection method and replating, a
232 significant number of white colonies for all four sgRNA variants were observed. Editing
233 efficiencies (determined as the ratio of white to red colonies) ranged from $3.4 \pm 2.7\%$ to
234 $46.2 \pm 22.2\%$ (Fig. 3A). Notably, these levels of editing efficiency are substantially higher
235 for *CAR2* than for any of the *URA3* targeting constructs, indicating that this genome region
236 is more amenable to Cas9-based genome editing. Furthermore, successful disruption of
237 *CAR2* indicates that multiplexed gene editing might be possible by selecting for *5-FOA^R*
238 colonies that exhibit a white phenotype.

239 To explore multiplexed deletion of two genes in *R. toruloides*, a Cas9 construct
240 targeting both *URA3* and *CAR2* was created. For this, multiple sgRNAs were placed
241 together sequentially into an array, with each guide RNA separated by a tRNA sequence
242 (Fig. 3B). This approach has been applied in other organisms to take advantage of
243 inherent tRNA post-transcriptional processing to express multiple unique sgRNA
244 sequences (42, 44, 45). Combining multiple sgRNAs in an array is particularly useful for

245 *R. toruloides*, as this minimizes the amount of genetic material that needs to be delivered
246 while maximizing the number of potential gene targets. Additionally, utilizing multiple
247 sgRNAs to target one gene at different locations allows for the possibility of removing a
248 large DNA in between the target sites, and also increases the possibility that the target
249 gene is successfully disrupted (20, 46, 47). Therefore, our constructs were designed to
250 express four sgRNAs (two for each gene) such that cleavage would occur at two sites
251 separated by ~500bp in both genes.

252 The multiplexed CRISPR editing construct fragment was transformed into *R.*
253 *toruloides* and multiple NAT^R colonies were selected to screen for genetic disruptions. To
254 determine loss of *CAR2* function, we grew colonies overnight in liquid cultures, which
255 were subsequently plated on Nat plates. Colonies were then screened for their red or
256 white phenotypes. This provided an estimate of the editing efficiency of *CAR2*, which
257 was determined to be $3.2\% \pm 0.5\%$, independently of the editing efficiency of *URA3*. To
258 determine loss of *URA3* function, an equal volume of each culture was plated on both Nat
259 and 5-FOA plates and the CFU counts on each plate were compared. This provided an
260 estimate of the editing efficiency of *URA3* of $1.1\% \pm 0.8\%$. Colonies growing on 5-FOA
261 were also screened for their red or white phenotypes to determine the dual-gene
262 disruption efficiency. Of the 5-FOA^R colonies, $30.0\% \pm 8.0\%$ exhibited a white phenotype,
263 indicating simultaneous *CAR2* and *URA3* disruption. A representative example of a 5-
264 FOA plate demonstrates the screening of dual-gene disruption (Fig. 3C).

265 We next sought to confirm that these edits were indeed the result of successful
266 Cas9-mediated editing. For this, eight white colonies were selected from the 5-FOA plates
267 and the regions of *URA3* and *CAR2* which surrounded the Cas9 target sites were PCR

268 amplified. Gel electrophoresis of these PCR products revealed that several of the
269 samples reduced significantly in size from the predicted size of the wildtype PCR products
270 (717nt and 1637nt for *URA3* and *CAR2* respectively) (Fig. 3 D, E).

271 Sequence-verification of these fragments was employed around the target cut sites
272 to see what type of gene editing events occurred (Fig. 3 F, G). Sequencing revealed that
273 most of the cut sites contained indels resulting in frameshift mutations. Cas9-based gene
274 editing was observed at both target sites for each gene in seven out of eight replicates.
275 Replicates three and eight demonstrated complete excision of the intergenic region
276 between both cut sites, while replicate four surprisingly demonstrated re-integration of the
277 intergenic region in its reverse direction. Similarly, editing of *CAR2* occurred in every
278 sample at cut site three, and at cut site four in all samples excluding replicates three, six,
279 and seven. Replicates four, five, and eight demonstrated complete removal of the
280 intergenic region between both cut sites. Again, replicates one and two demonstrated the
281 surprising evidence of re-integration of the reverse direction of the intergenic region.
282 Taken together, these results demonstrate that multiplexed gene disruption mediated by
283 CRISPR-Cas9 is possible in a single transformation of *R. toruloides*.

284 **DISCUSSION**

285 The development of CRISPR-Cas9 technology has revolutionized genome
286 engineering. Scientists are now able to rapidly edit the DNA of organisms where genetic
287 manipulation was previously inefficient or intractable (48). The fundamental science
288 underlying CRISPR engineering of genomes remains constant regardless of the organism
289 being investigated; scientists use these nucleases to induce DNA cuts at highly specific
290 locations and rely upon the organism's DNA repair machinery to mend these breaks with
291 donor DNA (via HR) or in an error-prone fashion (via NHEJ). However, the process of
292 delivering and expressing fully functional CRISPR components, and the biology of each
293 organism's DNA repair pathways, requires organism-specific optimization to
294 accommodate each species' unique characteristics. The past two years have seen the
295 publication of a wide array of studies demonstrating CRISPR-Cas9 genome engineering
296 in fungal species for which few robust DNA editing tools existed, including *Aspergillus*
297 *niger* (49), *Cryptococcus neoformans* (50), *Mucor circinelloides* (51), and *Myceliophthora*
298 *thermophila* (47). The dawning of a "fungal CRISPR revolution" has occurred,
299 empowering researchers to explore new bioproduction possibilities in obscure yet
300 promising fungi.

301 Here we add *R. toruloides* to the list of fungi now editable using CRISPR-Cas9.
302 While this yeast has been touted for its great bioproduction potential, the sparse genetic
303 manipulation toolkit relative to other organisms such as *Y. lipolytica* (27) previously
304 hindered engineering efforts (52–55). The past four years have seen various researchers
305 remedy this problem with the development of tools for transforming *R. toruloides* and
306 efficiently expressing exogenous DNA (15, 56). While the toolkit has expanded to include

307 useful promoters (53), drug markers (11), and targeted gene editing methods (18),
308 CRISPR-Cas9 methods for advanced genome engineering have been lacking. This study
309 outlines the strategies by which researchers can employ multiplexed CRISPR-Cas9
310 genome editing to manipulate *R. toruloides*. These are the first steps to ultimately
311 achieving more sophisticated genome- or transcriptome-scale engineering of *R.*
312 *toruloides*, an important step towards fulfilling the organism's potential.

313 Accomplishing this required overcoming significant barriers. Most notably, the lack
314 of a plasmid capable of replicating in *R. toruloides* to express CRISPR constructs, the
315 most common method for employing CRISPR editing in other fungi (24), requires
316 alternative approaches to express the editing system. One approach to accomplish this
317 would be to directly transform fully assembled Cas9-sgRNA RNP complexes (50). Such
318 an approach has proven successful in the distant basidiomycete relative *Cryptococcus*
319 *neoformans* (50), suggesting that it may one day prove successful in *R. toruloides*. An
320 alternate approach involving the delivery of DNA coding for CRISPR machinery was
321 explored in this study. We demonstrated that stable genome integration of a Cas9-sgRNA
322 expression cassette using a dominant selectable drug marker is sufficient to achieve gene
323 disruption.

324 The next major barrier we overcame was the successful expression of sgRNAs
325 intracellularly. This requires a robust RNA Pol-III promoter in order to achieve high
326 expression of the guides inside of the nucleus. *R. toruloides*, like many other non-model
327 fungi, have poorly explored Pol-III promoter systems (57). We therefore explored a variety
328 of such promoters, as well as RNA processing elements including ribozymes and self-
329 splicing tRNAs. We found the optimal sgRNA expression system to be tRNA-driven

330 guides, preferably using designs guided from sgRNA prediction programs, such as
331 sgRNA Scorer (38). There is conflicting evidence in the literature as to whether inclusion
332 of a ribozyme element improves sgRNA expression, with some studies finding that it
333 increases editing efficiency (35, 40) while others find the opposite effect (58). Here, our
334 results indicate that ribozyme inclusion is detrimental to Cas9 editing efficiency in *R.*
335 *toruloides*. Additionally, we demonstrated that multiple functional sgRNAs can be
336 expressed from a single construct using the tRNA processing system described in
337 previous works (44, 45). The low level of editing efficiency in this multiplexed sgRNA
338 design, relative to the editing efficiency levels of the sgRNAs expressed independently
339 (especially *CAR2* sgRNAs), indicates that further optimization of this design could
340 enhance multiplexed gene editing. This could include ensuring high-levels of endogenous
341 expression and efficient processing of the transcript into individual sgRNAs. While the
342 potential for optimization remains, our work towards optimized sgRNA expression
343 provides design guidelines for future CRISPR engineering efforts in *R. toruloides*.

344 A significant locus-dependent editing efficiency was observed in our study. Despite
345 much of our work focusing on optimization of *URA3* deletion with Cas9, we achieved a
346 relatively low maximum editing efficiency at this locus of 0.62% \pm 0.50%. However,
347 deletion of *CAR2* was markedly more successful in even the worst-case scenario (3.4%
348 \pm 2.7%), while the best-case scenario resulted in roughly a one-to-one ratio of white to
349 red colonies. The locus-dependency of Cas9 editing efficiency has been noted in other
350 non-yeast eukaryotic systems (23, 59, 60). Combined with the qualitatively large
351 differences observed between editing efficiencies of Cas9 at various *URA3* target
352 locations, optimization of the Cas9 target sequence appears to be particularly important

353 for editing in *R. toruloides*. Transient Cas9 binding events are known to occur much more
354 frequently than actual cleavage occurs, and changes in the protein's conformation upon
355 binding to the correct target sequence dictate whether DNA cutting actually occurs (61).
356 Furthermore, the high GC content of the *R. toruloides* genome should be taken into
357 consideration (62). A correlation between high GC content and lower Cas9 target
358 specificity has been noted (63), raising the possibility that Cas9 cleavage in *R. toruloides*
359 is (i) more promiscuous or (ii) less effective. A thorough exploration of genome editing
360 efficiencies of Cas9 at various locations in *R. toruloides*' genome would assist in future
361 genome editing endeavors in the organism.

362 The ability to achieve multiple DNA edits in one round of transformation is an
363 important step forward in *R. toruloides* genome engineering. Thus far, multiple gene edits
364 have been accomplished utilizing multiple rounds of ATMT in which genes are disrupted
365 one at a time; here we have demonstrated that four simultaneous DNA edits can be
366 achieved at once. The sgRNA array could theoretically be expanded to include even more
367 targets. It should be noted that a reduction in editing efficiency may occur with sgRNAs
368 located further downstream in the array. This is supported by the fact that the editing
369 efficiency of *URA3* deletion was relatively similar in the individual and multiplexed
370 targeting constructs (where the targets were located upstream), but the editing efficiency
371 of *CAR2* deletion was substantially lower in the multiplexed targeting construct (where
372 the targets were located downstream) than in the individual targeting case. The
373 multiplexed targeting construct also reveals an interesting phenomenon in which excised
374 DNA between two nearby CRISPR cut sites was inverted and reinserted into the genome.
375 This is potentially due to the relatively high level of NHEJ in *R. toruloides* (15) and

376 indicates that genome integration of exogenous DNA at Cas9 cut-sites may be possible
377 if donor DNA can be supplied concurrently with Cas9 cleavage.

378 Taken together, our work lays the foundation for Cas9-mediated advanced
379 genome editing in *R. toruloides*. Future efforts could improve upon this framework by
380 employing directed integration of the Cas9 cassette into a specific genetic locus in a
381 $\Delta KU70$ background or on an ARS-based plasmid to circumvent problems arising from
382 random genome integration in the current strategy. Ultimately, these results should
383 enable rapid engineering of complex *R. toruloides* phenotypes, such as multi-gene
384 pathways to produce biofuels and bioproducts.

385 **MATERIALS AND METHODS**

386 **Strains and culture conditions**

387 The strain *R. toruloides* IFO0880 (obtained from Biological Resource Center, NITE
388 (NRBC)) was used as the wild type strain for all experiments. Liquid cultures of yeast
389 were grown in YPD (BD Difco) at 30°C and constant 200rpm shaking unless otherwise
390 noted. Solid YPD agar plates were used to grow yeast colonies at 30°C and
391 supplemented with the antibiotics nourseothricin (Werner Bioagents, 100 µg/mL) or 5-
392 fluoroorotic acid (Abcam, 1 mg/mL), or geneticin (VWR, 100 µg/mL) as appropriate.

393 For all cloning, *Escherichia coli* strains XL1-Blue or DH5α were used to propagate
394 plasmids. *E. coli* were grown in lysogeny broth (LB, BD Difco) at 37°C with 200rpm
395 shaking. Where appropriate, *E. coli* media was supplemented with 100 µg/mL ampicillin
396 (or 100 µg/mL carbenicillin in place of ampicillin) or 50 µg/mL kanamycin to maintain
397 plasmids.

398

399 **Plasmid construction**

400 The coding sequence of *Streptococcus pyogenes* spCas9 and the SV40 NLS
401 (PKKKRKV) were codon-optimized for expression in *R. toruloides* (GenScript), with a
402 (Gly)₃ linker included to connect the C-term of spCas9 to the NLS. The fusion protein was
403 placed under expression of the 800bp GAPDH promoter sequence and NOS terminator
404 sequence, which is known to promote strong gene expression in *R. toruloides* (2, 54).
405 The desired optimized sequences were synthesized by GenScript and sequence verified.
406 All plasmids were commercially synthesized excluding plasmids p213 and p227-233,
407 which were constructed in our lab as follows. Plasmid p213 was first constructed by

408 creating two PCR products from p90 using primers 100-103, and subsequently using In-
409 Fusion HD Cloning (Clontech) to stitch the PCR products together. Plasmids p227-233
410 were created from p213 using primers 104-117 in PCR reactions to create new sgRNA
411 target sequences in individual PCR products, which were subsequently circularized using
412 In-Fusion HD Cloning. A table of strains, plasmids, primers used in this study are in tables
413 S1-3 and are available from the JBEI Registry (<https://registry.jbei.org/>).

414

415 **Transforming DNA preparation**

416 DNA for transformation into *R. toruloides* was prepared from the aforementioned
417 *E. coli* plasmids. To integrate their corresponding Cas9-constructs into the genome,
418 plasmids p90-99 and p184-190 were digested with HindIII, while plasmids pGI103-132
419 were digested with NdeI. Digestion products were subsequently confirmed using gel
420 electrophoresis and purified using a PCR purification kit (DNA Clean & Concentrator,
421 Zymo Research). These purified products were used directly for transformation. An
422 alternative method was used to integrate the corresponding Cas9-constructs on plasmids
423 p213-233 into the genome. These plasmids were instead PCR amplified using primers
424 122 and 123 (Table S2), and the PCR products were subsequently confirmed using gel
425 electrophoresis and purified using a PCR purification kit. These purified PCR products
426 were used directly for transformation. Regardless of DNA preparation method,
427 approximately 500 ng of transforming DNA was used for transformation.

428

429 **Transformation**

430 Transformation was performed using a modified lithium acetate (LiAc) protocol
431 (14). An individual yeast colony was inoculated into 10 mL YPD medium and grown
432 overnight at 30°C with 200 rpm shaking. The following morning, the OD₆₀₀ of this seed
433 culture was measured and used to inoculate 10mL of fresh YPD to an OD₆₀₀ of 0.2. This
434 culture was grown for another four hours at 30°C with 200 rpm shaking to an OD₆₀₀ of
435 approximately 1.0. Cells were pelleted via centrifugation at 4000g for five minutes,
436 washed twice with 10 mL H₂O, and washed once with 10 mL 150mM LiAc (Millipore
437 Sigma) at pH 7.6, and resuspended in one mL 150mM LiAc. The pellet was then
438 transferred to 1.5mL microcentrifuge tubes, centrifuged at 8000g for one minute, and the
439 supernatant was removed using a pipette. The wet biomass was then resuspended in
440 240 µL 50% w/v PEG-4000 (Alfa Aesar), 54 µL 1.0M LiAc, 10 µL of pre-boiled salmon
441 sperm DNA (Invitrogen), and 56 µL of transforming DNA (~500ng of purified PCR
442 product). The viscous slurry was resuspended via pipetting and incubated at 30°C for 30
443 minutes, after which 34 µL of 1M dithiothreitol (Millipore Sigma) dissolved in DMSO was
444 added. The transformation was heat shocked at 37°C for 60 minutes, and subsequently
445 pelleted and washed with one mL YPD. The culture was then resuspended in two mL
446 YPD and incubated overnight at 30°C with 200rpm shaking. Cells were pelleted,
447 resuspended in 200 µL YPD, and plated on the appropriate selective media. Utilizing this
448 method to randomly integrate dsDNA via the NHEJ pathway into the *R. toruloides*
449 genome typically provides ~500 colonies, or a transformation efficiency of ~1000
450 transformants/ µg

451

452 **Determination of gene edits**

453 *R. toruloides* samples transformed with transforming DNA made from plasmids
454 p90-p99 were plated directly on YPD plates supplemented with 5-FOA and grown for
455 three to four days. Colony forming units were subsequently determined for each
456 transformation. Three transformations were performed for every construct and plated on
457 independent plates to acquire three biological replicates. Three control samples in which
458 no DNA was included in the transformation were also performed to determine the rate of
459 spontaneous 5-FOA resistance.

460 *R. toruloides* samples transformed with all other transforming DNA (derived from
461 plasmids 184-233 and pGI104-132) harboring a *NAT* selective marker were plated
462 directly on YPD plates supplemented with nourseothricin and grown for two to three days.
463 Three colonies were selected from each transformation and grown overnight. For
464 experiments designed to edit the *URA3* locus, serial dilutions of each culture were plated
465 on both YPD and YPD supplemented with 5-FOA and grown for three to four days. For
466 *CAR2* gene editing experiments, serial dilutions of each culture were plated on YPD. Total
467 colony forming units were determined from serial dilutions providing between 10-1000
468 countable colonies. Conversion of the red phenotype to white phenotype was used as a
469 proxy for successful editing of the *CAR2* gene to induce a loss of function mutation.

470 For sequencing, individual colonies were selected from 5-FOA plates and grown
471 overnight in YPD. For Figs. 1, S1 and S2, genomic DNA was prepared using a custom
472 protocol of DNA extraction. For this, 200 μ L of yeast culture of approximately 0.40 OD₆₀₀
473 were centrifuged at maximum speed and the supernatant was removed. Pellets were
474 resuspended in 100 μ L of 200mM LiOAc supplemented with 1% SDS and incubated for
475 15 minutes at 95°C. The samples were supplemented with 300 μ L of 96-100% EtOH,

476 vortexed thoroughly, and centrifuged at maximum speed for three minutes. The
477 supernatant was aspirated off, and the pellet was washed once with 70% EtOH. The pellet
478 was resuspended in 100 μ L H₂O and pelleted at maximum speed for 15 seconds. The
479 resulting supernatant containing genomic DNA was recovered for downstream
480 applications. All other genomic DNA was recovered from 100 mg of wet biomass (Quick-
481 DNA Fungal/Bacterial Kit, Zymo Research). Genomic DNA quality was examined by
482 running on an agarose gel, and high-quality DNA was used as a template for PCR. The
483 genomic region around the *URA3* or *CAR2* target sites (see Table S2 for primers) were
484 amplified via PCR and run on an agarose gel. PCR products were purified and submitted
485 for Sanger sequencing (Quintara Biosciences).

486 **ACKNOWLEDGMENTS**

487 This material is based upon work supported by the U.S. Department of Energy
488 (DOE), Office of Science. Preliminary work in this project establishing experimental
489 protocols was supported by the U.S. DOE, Office of Science, Office of Biological and
490 Environmental Research program under Award Number DE-SC-0012527 to J.M.S. and
491 A.P.A. Work conducted by the DOE Joint BioEnergy Institute was supported by the U.S.
492 DOE, Office of Science, Office of Biological and Environmental Research, through
493 contract DE-AC02-05CH11231. Additional funding was provided by the Toyota Motor
494 Corporation under grant number IQADA62820 to J.M.S. and A.P.A.

495 The authors declare no competing financial interests related to this work.

496 P.B.O. wrote the manuscript. M.I., P.B.O., and J.M.S. conceived and designed the
497 experiments. M.I. and J.M.S. designed CRISPR constructs. P.B.O. and M.I. performed
498 experiments and analyzed the data. All authors read, edited, and approved the final
499 manuscript.

500 REFERENCES

501

- 502 1. Li Y, Zhao Z (Kent), Bai F. 2007. High-density cultivation of
503 oleaginous yeast *Rhodospiridium toruloides* Y4 in fed-batch culture.
504 Enzyme Microb Technol 41:312–317.
505 <https://10.1016/j.enzmictec.2007.02.008>.
- 506 2. Yaegashi J, Kirby J, Ito M, Sun J, Dutta T, Mirsiaghi M, Sundstrom
507 ER, Rodriguez A, Baidoo E, Tanjore D, Pray T, Sale K, Singh S,
508 Keasling JD, Simmons BA, Singer SW, Magnuson JK, Arkin AP,
509 Skerker JM, Gladden JM. 2017. *Rhodospiridium toruloides*: A new
510 platform organism for conversion of lignocellulose into terpene
511 biofuels and bioproducts. Biotechnol Biofuels 10:1–13.
512 <https://10.1186/s13068-017-0927-5>.
- 513 3. Xu J, Liu D. 2017. Exploitation of genus *Rhodospiridium* for microbial
514 lipid production. World J Microbiol Biotechnol 33:1–13.
515 <https://10.1007/s11274-017-2225-6>.
- 516 4. Chaturvedi S, Bhattacharya A, Khare SK. 2018. Trends in oil
517 production from oleaginous yeast using biomass: biotechnological
518 potential and constraints. Appl Biochem Microbiol 54:361–369.
519 <https://10.1134/S000368381804004X>.

- 520 5. Singh G, Jawed A, Paul D, Bandyopadhyay KK, Kumari A, Haque S.
521 2016. Concomitant production of lipids and carotenoids in
522 *Rhodospiridium toruloides* under osmotic stress using response
523 surface methodology. *Front Microbiol* 7:1–13.
524 [https://10.3389/fmicb.2016.01686](https://doi.org/10.3389/fmicb.2016.01686).
- 525 6. Hu C, Zhao X, Zhao J, Wu S, Zhao ZK. 2009. Effects of biomass
526 hydrolysis by-products on oleaginous yeast *Rhodospiridium*
527 *toruloides*. *Bioresour Technol* 100:4843–4847.
528 [https://10.1016/j.biortech.2009.04.041](https://doi.org/10.1016/j.biortech.2009.04.041).
- 529 7. Huang Q, Wang Q, Gong Z, Jin G, Shen H, Xiao S, Xie H, Ye S,
530 Wang J, Zhao ZK. 2013. Effects of selected ionic liquids on lipid
531 production by the oleaginous yeast *Rhodospiridium toruloides*.
532 *Bioresour Technol* 130:339–344.
533 [https://10.1016/j.biortech.2012.12.022](https://doi.org/10.1016/j.biortech.2012.12.022).
- 534 8. Sundstrom E, Yaegashi J, Yan J, Masson F, Papa G, Rodriguez A,
535 Mirsiaghi M, Liang L, He Q, Tanjore D, Pray TR, Singh S, Simmons B,
536 Sun N, Magnuson J, Gladden J. 2018. Demonstrating a separation-
537 free process coupling ionic liquid pretreatment, saccharification, and
538 fermentation with: *Rhodospiridium toruloides* to produce advanced
539 biofuels. *Green Chem* 20:2870–2879. [https://10.1039/c8gc00518d](https://doi.org/10.1039/c8gc00518d).

- 540 9. Díaz T, Fillet S, Campoy S, Vázquez R, Viña J, Murillo J, Adrio JL.
541 2018. Combining evolutionary and metabolic engineering in
542 *Rhodospiridium toruloides* for lipid production with non-detoxified
543 wheat straw hydrolysates. *Appl Microbiol Biotechnol* 102:3287–3300.
544 [https://10.1007/s00253-018-8810-2](https://doi.org/10.1007/s00253-018-8810-2).
- 545 10. Marella ER, Holkenbrink C, Siewers V, Borodina I. 2018. Engineering
546 microbial fatty acid metabolism for biofuels and biochemicals. *Curr*
547 *Opin Biotechnol* 50:39–46. [https://10.1016/j.copbio.2017.10.002](https://doi.org/10.1016/j.copbio.2017.10.002).
- 548 11. Park Y, Nicaud J, Ledesma-amaro R. 2018. The engineering potential
549 of *Rhodospiridium toruloides* as a workhorse for biotechnological
550 applications. *Trends Biotechnol* 36:304–317.
551 [https://10.1016/j.tibtech.2017.10.013](https://doi.org/10.1016/j.tibtech.2017.10.013).
- 552 12. Ko JK, Lee SM. 2018. Advances in cellulosic conversion to fuels:
553 engineering yeasts for cellulosic bioethanol and biodiesel production.
554 *Curr Opin Biotechnol* 50:72–80. [https://10.1016/j.copbio.2017.11.007](https://doi.org/10.1016/j.copbio.2017.11.007).
- 555 13. Shi S, Zhao H. 2017. Metabolic engineering of oleaginous yeasts for
556 production of fuels and chemicals. *Front Microbiol* 8:1–16.
557 [https://10.3389/fmicb.2017.02185](https://doi.org/10.3389/fmicb.2017.02185).
- 558 14. Tsai YY, Ohashi T, Kanazawa T, Polburee P, Misaki R, Limtong S,
559 Fujiyama K. 2017. Development of a sufficient and effective procedure

- 560 for transformation of an oleaginous yeast, *Rhodospiridium toruloides*
561 DMKU3-TK16. *Curr Genet* 63:359–371. [https://10.1007/s00294-016-](https://10.1007/s00294-016-0629-8)
562 0629-8.
- 563 15. Liu H, Jiao X, Wang Y, Yang X, Sun W, Wang J, Zhang S, Zhao ZK.
564 2017. Fast and efficient genetic transformation of oleaginous yeast
565 *Rhodospiridium toruloides* by using electroporation. *FEMS Yeast Res*
566 17:1–11. <https://10.1093/femsyr/fox017>.
- 567 16. Lin X, Wang Y, Zhang S, Zhu Z, Zhou YJ, Yang F, Sun W, Wang X,
568 Zhao ZK. 2014. Functional integration of multiple genes into the
569 genome of the oleaginous yeast *Rhodospiridium toruloides*. *FEMS*
570 *Yeast Res* 14:547–555. <https://10.1111/1567-1364.12140>.
- 571 17. Coradetti ST, Pinel D, Geiselman GM, Ito M, Mondo SJ, Reilly MC,
572 Cheng Y-F, Bauer S, Grigoriev I V, Gladden JM, Simmons BA, Brem
573 RB, Arkin AP, Skerker JM. 2018. Functional genomics of lipid
574 metabolism in the oleaginous yeast *Rhodospiridium toruloides*. *Elife*
575 7:e32110. <https://10.7554/eLife.32110>.
- 576 18. Koh CMJ, Liu Y, Moehninsi, Du M, Ji L. 2014. Molecular
577 characterization of KU70 and KU80 homologues and exploitation of a
578 KU70-deficient mutant for improving gene deletion frequency in
579 *Rhodospiridium toruloides*. *BMC Microbiol* 14:53–68.

- 580 <https://10.1186/1471-2180-14-50>.
- 581 19. Zhang S, Ito M, Skerker JM, Arkin AP, Rao C V. 2016. Metabolic
582 engineering of the oleaginous yeast *Rhodospiridium toruloides*
583 IFO0880 for lipid overproduction during high-density fermentation.
584 *Appl Microbiol Biotechnol* 100:9393–9405. [https://10.1007/s00253-](https://10.1007/s00253-016-7815-y)
585 [016-7815-y](https://10.1007/s00253-016-7815-y).
- 586 20. Hsu PD, Lander ES, Zhang F. 2014. Development and applications of
587 CRISPR-Cas9 for genome engineering. *Cell* 157:1262–1278.
588 <https://10.1016/j.cell.2014.05.010>.
- 589 21. Ledford H. 2015. CRISPR, the disruptor. *Nature* 522:20–24.
590 <https://10.1038/522020a>.
- 591 22. Jinek M, Chylinski K, Fonfara I, Hauer M, Doudna JA, Charpentier E.
592 2012. A programmable dual-RNA-guided DNA endonuclease in
593 adaptive bacterial immunity. *Science* 337:816–821.
594 <https://10.1126/science.1225829>.
- 595 23. Langner T, Kamoun S, Belhaj K. 2018. CRISPR crops: plant genome
596 editing toward disease resistance. *Annu Rev Phytopathol* 56:479–512.
597 <https://10.1146/annurev-phyto-080417-050158>.
- 598 24. Shi TQ, Liu GN, Ji RY, Shi K, Song P, Ren LJ, Huang H, Ji XJ. 2017.
599 CRISPR/Cas9-based genome editing of the filamentous fungi: the

- 600 state of the art. *Appl Microbiol Biotechnol* 101:7435–7443.
- 601 [https://10.1007/s00253-017-8497-9](https://doi.org/10.1007/s00253-017-8497-9).
- 602 25. Deng H, Gao R, Liao X, Cai Y. 2017. CRISPR system in filamentous
603 fungi: Current achievements and future directions. *Gene* 627:212–
604 221. [https://10.1016/j.gene.2017.06.019](https://doi.org/10.1016/j.gene.2017.06.019).
- 605 26. Blazeck J, Hill A, Liu L, Knight R, Miller J, Pan A, Otoupal P, Alper HS.
606 2014. Harnessing *Yarrowia lipolytica* lipogenesis to create a platform
607 for lipid and biofuel production. *Nat Commun* 5:3131.
608 [https://10.1038/ncomms4131](https://doi.org/10.1038/ncomms4131).
- 609 27. Adrio JL. 2017. Oleaginous yeasts: Promising platforms for the
610 production of oleochemicals and biofuels. *Biotechnol Bioeng*
611 114:1915–1920. [https://10.1002/bit.26337](https://doi.org/10.1002/bit.26337).
- 612 28. Liu L, Otoupal P, Pan A, Alper HS. 2014. Increasing expression level
613 and copy number of a *Yarrowia lipolytica* plasmid through regulated
614 centromere function. *FEMS Yeast Res* [https://10.1111/1567-](https://doi.org/10.1111/1567-1364.12201)
615 1364.12201.
- 616 29. Markham KA, Alper HS. 2018. Synthetic Biology Expands the
617 Industrial Potential of *Yarrowia lipolytica*. *Trends Biotechnol* 1–11.
618 [https://10.1016/j.tibtech.2018.05.004](https://doi.org/10.1016/j.tibtech.2018.05.004).
- 619 30. Zetsche B, Heidenreich M, Mohanraju P, Fedorova I, Kneppers J,

- 620 Degennaro EM, Winblad N, Choudhury SR, Abudayyeh OO,
621 Gootenberg JS, Wu WY, Scott DA, Severinov K, Van Der Oost J,
622 Zhang F. 2017. Multiplex gene editing by CRISPR-Cpf1 using a single
623 crRNA array. *Nat Biotechnol* 35:31–34. <https://10.1038/nbt.3737>.
- 624 31. Verwaal R, Buiting-Wiessenhaan N, Dalhuijsen S, Roubos JA. 2018.
625 CRISPR/Cpf1 enables fast and simple genome editing of
626 *Saccharomyces cerevisiae*. *YEAST* 35:201–211.
627 <https://10.1002/yea.3278>.
- 628 32. Krappmann S. 2007. Gene targeting in filamentous fungi: the benefits
629 of impaired repair. *Fungal Biol Rev* 21:25–29.
630 <https://10.1016/j.fbr.2007.02.004>.
- 631 33. Dicarlo JE, Norville JE, Mali P, Rios X, Aach J, Church GM. 2013.
632 Genome engineering in *Saccharomyces cerevisiae* using CRISPR-
633 Cas systems. *Nucleic Acids Res* 41:4336–4343.
634 <https://10.1093/nar/gkt135>.
- 635 34. Krappmann S. 2017. CRISPR-Cas9, the new kid on the block of
636 fungal molecular biology. *Med Mycol* 55:16–23.
637 <https://10.1093/mmy/myw097>.
- 638 35. Ryan OW, Skerker JM, Maurer MJ, Li X, Tsai JC, Poddar S, Lee ME,
639 DeLoache W, Dueber JE, Arkin AP, Cate JHD. 2014. Selection of

- 640 chromosomal DNA libraries using a multiplex CRISPR system. *Elife*
641 3:1–15. [https://10.7554/eLife.03703](https://doi.org/10.7554/eLife.03703).
- 642 36. Alani E, Cao L, Kleckner N. 1987. A method for gene disruption that
643 allows repeated use of *URA3* selection in the construction of multiply
644 disrupted yeast strains. *Genetics* 116:541–545.
645 [https://10.1534/genetics.112.541.test](https://doi.org/10.1534/genetics.112.541.test).
- 646 37. Radzsheuskaya A, Shlyueva D, Müller I, Helin K. 2016. Optimizing
647 sgRNA position markedly improves the efficiency of CRISPR/dCas9-
648 mediated transcriptional repression. *Nucleic Acids Res* 44.
649 [https://10.1093/nar/gkw583](https://doi.org/10.1093/nar/gkw583).
- 650 38. Chari R, Yeo NC, Chavez A, Church GM. 2017. SgRNA Scorer 2.0: a
651 species-independent model to predict CRISPR/Cas9 activity. *ACS*
652 *Synth Biol* 6:902–904. [https://10.1021/acssynbio.6b00343](https://doi.org/10.1021/acssynbio.6b00343).
- 653 39. Braman JC. 2018. *Synthetic Biology Methods and Protocols* Methods
654 in Molecular Biology.
- 655 40. de Vries ARG, de Groot PA, van den Broek M, Daran JMG. 2017.
656 CRISPR-Cas9 mediated gene deletions in lager yeast
657 *Saccharomyces pastorianus*. *Microb Cell Fact* 16:1–18.
658 [https://10.1186/s12934-017-0835-1](https://doi.org/10.1186/s12934-017-0835-1).
- 659 41. Schwartz CM, Hussain MS, Blenner M, Wheeldon I. 2016. Synthetic

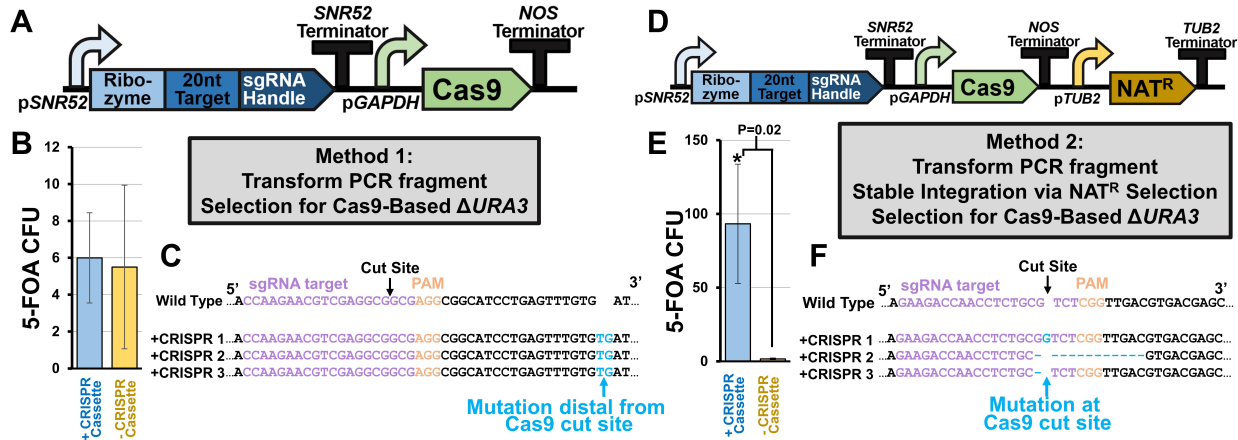
- 660 RNA Polymerase III Promoters Facilitate High-Efficiency CRISPR-
661 Cas9-Mediated Genome Editing in *Yarrowia lipolytica*. *ACS Synth Biol*
662 5:356–359. <https://10.1021/acssynbio.5b00162>.
- 663 42. Song L, Ouedraogo JP, Kolbusz M, Nguyen TTM, Tsang A. 2018.
664 Efficient genome editing using tRNA promoter-driven CRISPR/Cas9
665 gRNA in *Aspergillus Niger*. *PLoS One* 13:1–17.
666 <https://10.1371/journal.pone.0202868>.
- 667 43. Landolfo S, Ianiri G, Camiolo S, Porceddu A, Mulas G, Chessa R,
668 Zara G, Mannazzu I. 2018. CAR gene cluster and transcript levels of
669 carotenogenic genes in *Rhodotorula mucilaginosa*. *Microbiol (United*
670 *Kingdom)* 164:78–87. <https://10.1099/mic.0.000588>.
- 671 44. Xie K, Minkenberg B, Yang Y. 2015. Boosting CRISPR/Cas9 multiplex
672 editing capability with the endogenous tRNA-processing system. *Proc*
673 *Natl Acad Sci* 112:3570–3575. <https://10.1073/pnas.1420294112>.
- 674 45. Nødvig CS, Hoof JB, Kogle ME, Jarczynska ZD, Lehmbeck J,
675 Klitgaard DK, Mortensen UH. 2018. Efficient oligo nucleotide mediated
676 CRISPR-Cas9 gene editing in *Aspergilli*. *Fungal Genet Biol* 115:78–
677 89. <https://10.1016/j.fgb.2018.01.004>.
- 678 46. Wang H, Yang H, Shivalila CS, Dawlaty MM, Cheng AW, Zhang F,
679 Jaenisch R. 2013. One-step generation of mice carrying mutations in

- 680 multiple genes by CRISPR/cas-mediated genome engineering. *Cell*
681 153:910–918. [https://10.1016/j.cell.2013.04.025](https://doi.org/10.1016/j.cell.2013.04.025).
- 682 47. Liu Q, Gao R, Li J, Lin L, Zhao J, Sun W, Tian C. 2017. Development
683 of a genome-editing CRISPR/Cas9 system in thermophilic fungal
684 *Myceliophthora* species and its application to hyper-cellulase
685 production strain engineering. *Biotechnol Biofuels* 10:1–14.
686 [https://10.1186/s13068-016-0693-9](https://doi.org/10.1186/s13068-016-0693-9).
- 687 48. Ran FA, Hsu PD, Wright J, Agarwala V, Scott DA, Zhang F. 2013.
688 Genome engineering using the CRISPR-Cas9 system. *Nat Protoc*
689 8:2281–2308. [https://10.1038/nprot.2013.143](https://doi.org/10.1038/nprot.2013.143).
- 690 49. Sarkari P, Marx H, Blumhoff ML, Mattanovich D, Sauer M, Steiger
691 MG. 2017. An efficient tool for metabolic pathway construction and
692 gene integration for *Aspergillus niger*. *Bioresour Technol* 245:1327–
693 1333. [https://10.1016/j.biortech.2017.05.004](https://doi.org/10.1016/j.biortech.2017.05.004).
- 694 50. Wang P. 2018. Two distinct approaches for CRISPR-Cas9-mediated
695 gene editing in *Cryptococcus neoformans* and related species.
696 *mSphere* 3:e00208-18. [https://10.1128/mSphereDirect.00208-18](https://doi.org/10.1128/mSphereDirect.00208-18).
- 697 51. Nagy G, Szebenyi C, Csernetics Á, Vaz AG, Tóth EJ, Vágvölgyi C,
698 Papp T. 2017. Development of a plasmid free CRISPR-Cas9 system
699 for the genetic modification of *Mucor circinelloides*. *Sci Rep* 7:1–10.

- 700 <https://10.1038/s41598-017-17118-2>.
- 701 52. Sun W, Yang X, Wang X, Jiao X, Zhang S, Luan Y, Zhao ZK. 2018.
702 Developing a flippase-mediated marker recycling protocol for the
703 oleaginous yeast *Rhodospiridium toruloides*. *Biotechnol Lett* 40:933–
704 940. <https://10.1007/s10529-018-2542-3>.
- 705 53. Johns AMB, Love J, Aves SJ. 2016. Four inducible promoters for
706 controlled gene expression in the oleaginous yeast *Rhodotorula*
707 *toruloides*. *Front Microbiol* 7:1585. <https://10.3389/fmicb.2016.01666>.
- 708 54. Liu Y, Koh CMJ, Sun L, Hlaing MM, Du M, Peng N, Ji L. 2013.
709 Characterization of glyceraldehyde-3-phosphate dehydrogenase gene
710 RtGPD1 and development of genetic transformation method by
711 dominant selection in oleaginous yeast *Rhodospiridium toruloides*.
712 *Appl Microbiol Biotechnol* 97:719–729. [https://10.1007/s00253-012-](https://10.1007/s00253-012-4223-9)
713 [4223-9](https://10.1007/s00253-012-4223-9).
- 714 55. Wang Y, Lin X, Zhang S, Sun W, Ma S, Zhao ZK. 2016. Cloning and
715 evaluation of different constitutive promoters in the oleaginous yeast
716 *Rhodospiridium toruloides*. *Yeast* 33:99–106.
717 <https://10.1002/yea.3145>.
- 718 56. Liu Y, Yap SA, Koh CMJ, Ji L. 2016. Developing a set of strong
719 intronic promoters for robust metabolic engineering in oleaginous

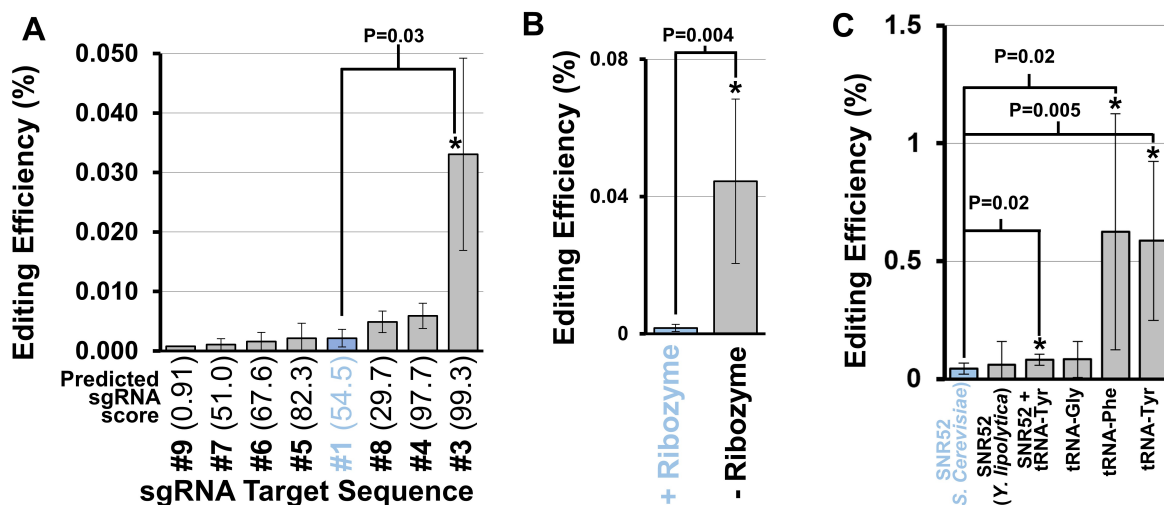
- 720 *Rhodotorula (Rhodosporidium)* yeast species. *Microb Cell Fact* 15:1–
721 9. <https://10.1186/s12934-016-0600-x>.
- 722 57. Morse NJ, Wagner JM, Reed KB, Gopal MR, Lauffer LH, Alper HS.
723 2018. T7 polymerase expression of guide RNAs *in vivo* allows
724 exportable CRISPR-Cas9 editing in multiple yeast hosts. *ACS Synth*
725 *Biol* 7:1075–1084. <https://10.1021/acssynbio.7b00461>.
- 726 58. Apel AR, D’Espaux L, Wehrs M, Sachs D, Li RA, Tong GJ, Garber M,
727 Nnadi O, Zhuang W, Hillson NJ, Keasling JD, Mukhopadhyay A. 2017.
728 A Cas9-based toolkit to program gene expression in *Saccharomyces*
729 *cerevisiae*. *Nucleic Acids Res* 45:496–508.
730 <https://10.1093/nar/gkw1023>.
- 731 59. Hsu PD, Scott D a, Weinstein J a, Ran FA, Konermann S, Agarwala
732 V, Li Y, Fine EJ, Wu X, Shalem O, Cradick TJ, Marraffini L a, Bao G,
733 Zhang F. 2013. DNA targeting specificity of RNA-guided Cas9
734 nucleases. *Nat Biotechnol* 31:827–32. <https://10.1038/nbt.2647>.
- 735 60. Merkle FT, Neuhausser WM, Santos D, Valen E, Gagnon JA, Maas K,
736 Sandoe J, Schier AF, Eggan K. 2015. Efficient CRISPR-Cas9-
737 mediated generation of knockin human pluripotent stem cells lacking
738 undesired mutations at the targeted locus. *Cell Rep* 11:875–883.
739 <https://10.1016/j.celrep.2015.04.007>.

- 740 61. Sternberg SH, Lafrance B, Kaplan M, Doudna JA. 2015.
741 Conformational control of DNA target cleavage by CRISPR-Cas9.
742 Nature 527:110–113. <https://10.1038/nature15544>.
- 743 62. Sambles C, Middelhaufe S, Soanes D, Kolak D, Lux T, Moore K,
744 Matoušková P, Parker D, Lee R, Love J, Aves SJ. 2017. Genome
745 sequence of the oleaginous yeast *Rhodotorula toruloides* strain
746 CGMCC 2.1609. Genomics Data 13:1–2.
747 <https://10.1016/j.gdata.2017.05.009>.
- 748 63. Tsai SQ, Zheng Z, Nguyen NT, Liebers M, Topkar V V., Thapar V,
749 Wyvekens N, Khayter C, Iafrate AJ, Le LP, Aryee MJ, Joung JK.
750 2015. GUIDE-seq enables genome-wide profiling of off-target
751 cleavage by CRISPR-Cas nucleases. Nat Biotechnol 33:187–198.
752 <https://10.1038/nbt.3117>.
753



754

755 **FIG 1** Targeted gene disruption using CRISPR-Cas9. (A) Schematic of original CRISPR-
 756 Cas9 design for causing indels in *R. toruloides*. A PCR fragment containing the coding
 757 sequences for expressing sgRNA and Cas9 is transformed into competent cells, which
 758 uptake the DNA into their nucleus and express the machinery from the PCR fragment.
 759 (B) Total colony forming units (CFU) of *R. toruloides* under 5-FOA selection with and
 760 without application of this CRISPR-Cas9 editing scheme. (C) Partial sequencing of *URA3*
 761 of each potentially edited colony near the cut site of Cas9. (D) Revised protocol in which
 762 the coding sequence for a selectable marker is included in the PCR fragment and an
 763 additional selection step for integration of the fragment into the genome is included. (E)
 764 Total CFU of *R. toruloides* under 5-FOA selection with this revised CRISPR-Cas9 editing
 765 scheme. Significance was calculated using a two-tailed type II student's *t*-test. (F) Partial
 766 sequencing of *URA3* of three edited colonies near the cut site of Cas9. All error bars
 767 represent the standard deviation of biological triplicates.



768

769 **FIG 2** Optimization of sgRNA expression and target sequence. (A) Editing efficiency of

770 various sgRNA target sequences. Bars indicate measured CRISPR-Cas9 gene editing

771 efficiency, as a percentage of the total cells in the transformation mixture exhibiting the

772 expected edited phenotype. Significant differences from the original target sequence

773 (highlighted in blue, $P < 0.05$) is indicated by asterisks and calculated using a two-tailed

774 type II student's t -test. The predicted aptitude for a target sequence to achieve successful

775 DNA editing based on the sgRNA Scorer 2.0 algorithm (38) is depicted in parentheses

776 after each target sequence. (B) Measured editing efficiency of sgRNA with and without

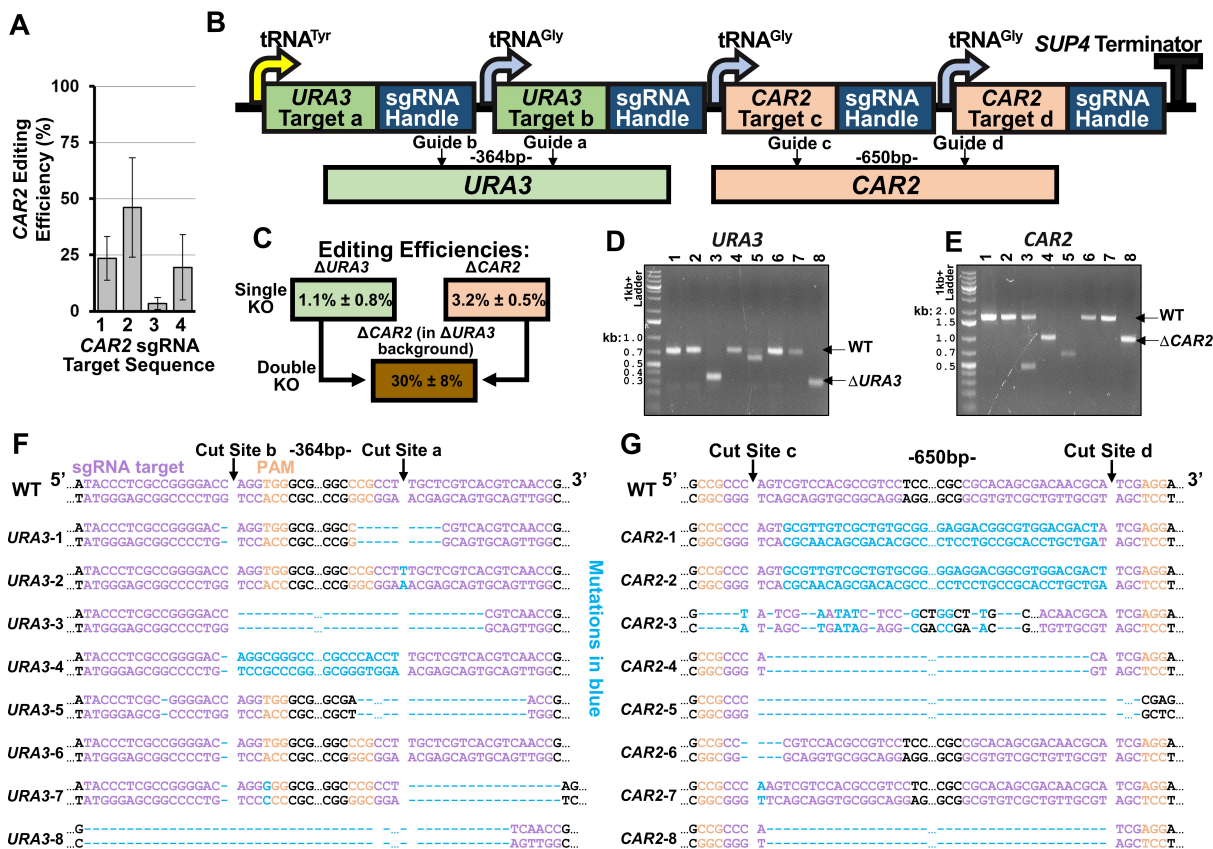
777 an HDV ribozyme cleavage site included between the promoter and the 20 nt target

778 sequence. (C) Measured editing efficiency of various promoters used to drive sgRNA

779 expression. All asterisks indicate statistical difference from the original expression design

780 (highlighted in blue, $P < 0.05$) calculated using a two-tailed type II student's t -test. Error

781 bars represent the standard deviation of biological triplicates.



782

783 **FIG 3** Multiplexed gene disruption using CRISPR-Cas9 in *R. toruloides*. (A) Editing

784 efficiency of four sgRNAs targeting *CAR2*. Error bars represent standard deviations of

785 biological triplicates. (B) The design used to express multiple sgRNAs in a single array.

786 The specific cut sites for *URA3* and *CAR2* are shown below. Guides “a” and “b”

787 correspond to sgRNAs “4” and “3” for *URA3*, while guides “c” and “d” correspond to

788 sgRNAs “1” and “3” for *CAR2* based on the sequences presented in Table S3. (C) 5-FOA

789 plate with colonies demonstrating successful simultaneous disruption of both genes. To

790 the right is shown the editing efficiency of disrupting each gene individually, as well as

791 tandem gene-disruption editing efficiency. (D, E) Gel image showing PCR amplification

792 of genomic DNA of eight unique colonies near the targeted cut site of (D) *URA3* or (E)

793 *CAR2*. (F) Sequencing results near the target cut site of the eight *URA3* PCR products

794 from (D). Cas9 cut sites are indicated, as well as the DNA size of the excised DNA
795 fragment between each cut site. Mutations are highlighted in blue. (G) Sequencing results
796 near the target cut site of the eight *CAR2* PCR products from (E). Mutations caused by
797 Cas9 targeting are highlighted in blue. All error bars represent standard deviation of
798 biological triplicates.